Inorganic Chemistry

Article

pubs.acs.org/IC

Zinc(II) and Cadmium(II) Monohydroxide Bridged, Dinuclear Metallacycles: A Unique Case of Concerted Double Berry Pseudorotation

Daniel L. Reger,* Andrea E. Pascui, Perry J. Pellechia, and Mark D. Smith

Department of Chemistry and Biochemistry, University of South Carolina, Columbia, South Carolina 29208, United States

Web-Enhanced Feature *Supporting Information*

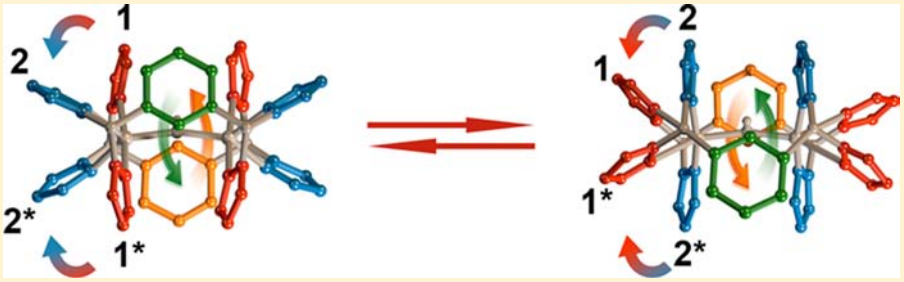

ABSTRACT: The reactions of $M(ClO_4)_2 \cdot 6H_2O$ [M = Zn(II), Cd(II)] and the ligands *m*-bis[bis(1-pyrazolyl)methyl]benzene, $\mathbf{L}_m$, or *m*-bis[bis(3,5-dimethyl-1-pyrazolyl)methyl]benzene, $\mathbf{L}_m$*, in the presence of a base yield the hydroxide bridged dinuclear metallacycles $[M_2(\mu\text{-OH})(\mu\text{-L})_2](ClO_4)_3$, **L** = $\mathbf{L}_m$, M = Zn(II) (**1**); **L** = $\mathbf{L}_m$*, M = Zn(II) (**2**), Cd(II) (**3**). In the solid state, the coordination environment of the metals is distorted trigonal bipyramidal with the bridging hydroxide in an equatorial position and M-O-M angles greater than 161°. The observation of two equal intensity resonances for each type of pyrazolyl-ring hydrogen in the ^{1}H NMR for all three complexes coupled with the determination of the hydrodynamic radius based on the diffusion coefficient of **1** that matches that observed in the crystal structure, demonstrate this structure is retained in solution. Additional proof of the dinuclear structures in solution is given by the ^{113}Cd NMR spectrum of $[Cd_2(\mu\text{-OH})(\mu\text{-}\mathbf{L}_m{}^*)_2](ClO_4)_3$ showing $^{111/113}$Cd satellites ($J^{111}_{Cd\text{-}}{}^{113}_{Cd}$ = 173 Hz). Complex **1** is dynamic in solution, with the resonances for each type of pyrazolyl-ring hydrogen broadening and averaging at higher temperatures. Detailed variable temperature studies show that $\Delta G_{pz}{}^{\ddagger}$ = 15.2(±0.2) kcal/mol, $\Delta H_{pz}{}^{\ddagger}$ = 6.6(±0.1) kcal/mol, and $\Delta S_{pz}{}^{\ddagger}$ = −28.8(±0.4) cal/mol·K at 25 °C for this process. The same $\Delta G^{\ddagger}$ value for the dynamic process was also determined by saturation transfer experiments. The most plausible mechanism for this dynamic process, which exchanges the axial and equatorial positions of the pyrazolyl rings in the trigonal bipyramidal arrangement, involves Berry pseudorotation at *both metal sites* using the bridging oxygen atom as the pivot ligand, coupled with the ring flip of the ligand's phenylene spacer by 180°, a rearrangement process we termed the "Columbia Twist and Flip". This process was shown to be influenced by trace amounts of water in the solvent, with a linear relationship between the water concentration and $\Delta G_{pz}{}^{\ddagger}$; increasing the water concentration lowers $\Delta G_{pz}{}^{\ddagger}$. Spin saturation transfer experiments demonstrated the exchange of the hydrogens between the water in the solvent and the bridging hydroxide group, with $\Delta G_{OH}{}^{\ddagger}$ = 16.8(±0.2) kcal/mol at 25 °C, a value larger than the barrier of $\Delta G_{pz}{}^{\ddagger}$ = 15.2(±0.2) kcal/mol for the "Columbia Twist and Flip". Compounds **2** and **3** do not show dynamic behavior involving the pyrazolyl-rings in solution because of steric crowding caused by the methyl group substitution, but do show the exchange between the water in the solvent and the bridging hydroxide group.

1. INTRODUCTION

The structure and molecular motion of self-assembled complexes of diamagnetic metal centers are of considerable interest.[1] The quest for the creation of artificial molecular machineries stimulated the design and synthesis of numerous organic molecules that resemble macroscopic machineries, such as rotors, motors, and gyroscopes.[2] Recently it was proposed that metal−organic frameworks (MOFs) and discrete metallacyclic rotors might have superior properties compared to the more conventional organic rotors, in the sense that the conformational dynamics can be easily controlled using supramolecular metal-directed approaches.[3] Garcia-Garibay and co-workers recently studied the lattice dynamics of MOF-5, $Zn_4O(BDC\text{-}NH_2)_3$ (BDC = 1,4-benzenedicarboxylate), with the goal to control the internal dynamics of such systems, which ultimately "may open opportunities for the development of functional materials and artificial molecular machines".[4] In addition, there is major interest in the structure and solution behavior of zinc(II) and cadmium(II) hydroxide bridged dinuclear systems,[5] which stems from the existence of similar units in several dinuclear metallohydrolases.[6]

Over the past years we gained significant understanding of the solid state structure and magnetostructural correlations in

Received: August 12, 2013
Published: September 9, 2013

single anion (F^-, Cl^-, Br^-, OH^-) bridged dinuclear metallacycles supported by bis(pyrazolyl)methane ligands, $\mathbf{L}_m$, *m*-bis[bis(1-pyrazolyl)methyl]benzene and $\mathbf{L}_m$*, *m*-bis[bis(3,5-dimethyl-1-pyrazolyl)methyl]benzene (Scheme 1).[7,8] Herein

Scheme 1. Schematic Drawing of the Structure of $\mathbf{L}_m$ and $\mathbf{L}_m$*[a]

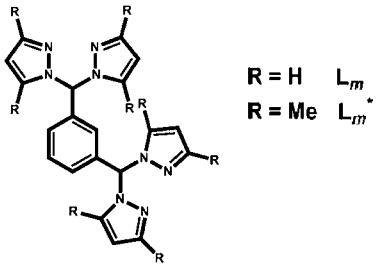

[a]The ligands contain two bis(pyrazolyl)methane units connected by a 1,3-phenylene spacer.

we report the synthesis, structure (both in solid state and solution) of three monohydroxide bridged metallacycles with these bis(pyrazolyl)methane ligands, and the complex molecular motion of these compounds in solution, as studied by ^{1}H variable temperature (VT) NMR and saturation transfer experiments. We highlight the effect of trace amounts of water in the solvent and the impact of methyl-substitution of the ligand on the conformational dynamics of the system.

2. EXPERIMENTAL SECTION

General Considerations. Standard Schlenk techniques were used for the synthesis of the hydroxide bridged compounds. The solvents were not dried prior to use. The ligands, $\mathbf{L}_m$[9] and $\mathbf{L}_m$*,[7a] were prepared following reported procedures. All other chemicals were purchased from Sigma-Aldrich or Strem Chemicals and used as received.

Crystals used for elemental analysis and mass spectrometry were removed from the mother liquor, rinsed with ether, and dried under vacuum, a process that removes the solvent of crystallization, if present.

^{1}H, ^{13}C, and ^{113}Cd NMR spectra were recorded on a Varian Mercury/VX 300, Varian Mercury/VX 400, or Varian INOVA 500 spectrometer. All chemical shifts are in ppm and were referenced to residual nondeuterated solvent signals (^{1}H), deuterated solvent signals (^{13}C), or externally to $CdCl_2$ (^{113}Cd). To test the accuracy of the saturation transfer experiment we used a sample of *N*,*N*-dimethylacetamide diluted in toluene-d_8, calculated k (rate constant), and $\Delta G^{\ddagger}$ for the rotational barrier about the amide bond. The calculated values (25.0 °C: k = 0.53 s^{-1}, $\Delta G^{\ddagger}$ = 17.8 kcal/mol) are comparable with literature values (22.5 °C: k = 0.61 s^{-1}, $\Delta G_{OH}^{\ddagger}$ = 17.7 kcal/mol).[10]

Mass spectrometric measurements were obtained on a MicroMass QTOF spectrometer in an acid-free environment. Elemental analyses were performed on vacuum-dried samples by Robertson Microlit Laboratories (Ledgewood, NJ).

XSEED,[11] POV-RAY,[11] and MESTRENOVA[12] were used for the preparation of figures.

Caution! *Although no problems were encountered during this work with the perchlorate salts, these compounds should be considered potentially explosive.*[13]

$[Zn_2(\mu\text{-}OH)(\mu\text{-}L_m)_2](ClO_4)_3$, 1. To a methanolic solution (10 mL) of the ligand $\mathbf{L}_m$ (0.19 g, 0.51 mmol), NEt_3 (0.07 mL, 0.5 mmol) was added. The $Zn(ClO_4)_2{\cdot}6H_2O$ (0.19 g, 0.51 mmol) was dissolved in 4 mL of methanol and the ligand/amine solution was transferred by cannula into the zinc(II) salt solution. A white precipitate formed immediately. The reaction mixture was stirred for 5 h. The crude product, 0.145 g (48%), was collected by cannula filtration, washed with 5 mL ether, and dried under vacuum overnight. Single crystals suitable for X-ray studies were grown by vapor diffusion of Et_2O into 1 mL acetonitrile solutions of **1** and were mounted directly from the mother liquor as **1**·CH_3CN (major form) and **1**·1.5CH_3CN (minor form). ^{1}H NMR (400 MHz, acetonitrile-d_3) at 20 °C: δ 8.40/8.19 (s/s, 4H/4H, 5-H pz) 8.15 (s, 4H, $CH(pz)_2$), 7.56 (t, J = 8.0 Hz, 2H, 5-H C_6H_4), 7.48/6.64 (s/s, 4H/4H, 3-H pz), 6.63 (d, J = 12.0 Hz, 4H, 4,6-H C_6H_4), 6.52/6.42 (s/s, 4H/4H, 4-H pz), 4.75 (s, 2H, 2-H C_6H_4), −0.66 (s, 1H, Zn−(O)H−Zn). ^{13}C NMR (100.6 MHz, acetonitrile-d_3) at 20 °C: δ 144.6 (broad, 3-C pz), 137.4 (1,3-C C_6H_4), 138.0/136.3 (5-C pz), 130.8 (5-C C_6H_4), 128.9 (4,6-C C_6H_4), 124.5 (2-C C_6H_4), 108.4 (4-H pz), 75.2 ($CH(pz)_2$). ^{13}C NMR (100.6 MHz, acetonitrile-d_3) at −40 °C: δ 143.7/142.9 (3-C pz), 136.2 (1,3-C C_6H_4), 137.0/135.2 (5-C pz), 129.5 (5-C C_6H_4), 128.0 (4,6-C C_6H_4), 123.6 (2-C C_6H_4), 107.1/107.0 (4-H pz), 73.8 ($CH(pz)_2$). Anal. Calcd.(Found) for $C_{40}H_{37}Cl_3Zn_2N_{16}O_{13}$: C, 40.49 (40.15); H, 3.14 (3.21); N, 18.88 (18.75). MS ES(+) *m*/*z* (rel. % abund.) [assgn]: 1087 (1) $[Zn_2(\mathbf{L}_m)_2(OH)(ClO_4)_2]^+$, 903 (13) $[Zn(\mathbf{L}_m)_2(ClO_4)]^+$, 533 (30) $[Zn_2(\mathbf{L}_m)_2(ClO_4)_2]^{2+}$, 494 (27) $[Zn_2(\mathbf{L}_m)_2(OH)(ClO_4)]^{2+}$, 451 (10) $[Zn\mathbf{L}_mOH]^+$, 402 (100) $[Zn(\mathbf{L}_m)_2]^{2+}$, 371 (19) $[\mathbf{L}_m + H]^+$, 296 (48) $[Zn_2(\mathbf{L}_m)_2(OH)]^{3+}$.

$[Zn_2(\mu\text{-}OH)(\mu\text{-}L_m^*)_2](ClO_4)_3$, 2. Compound **2** was prepared similarly to compound **1** starting from $\mathbf{L}_m$* (0.25 g, 0.51 mmol), NEt_3 (0.070 mL, 0.51 mmol), and $Zn(ClO_4)_2{\cdot}6H_2O$ (0.19 g, 0.51 mmol). The reaction afforded 0.100 g of a white precipitate. Single crystals were grown the same way as crystals of **1**. The samples of crystals of **2** are contaminated by a poorly crystalline material that was not identified, and from which it could not be separated. The NMR spectrum of these crystals of **2** indicates about 20% impurity, but the resonances of **2** can be assigned based on the NMR spectra of **1**, **3**, and related compounds. ^{1}H NMR (300 MHz, acetonitrile-d_3) at 20 °C: δ 7.68 (s, 4H, $CH(pz)_2$), 7.59 (t, J = 12 Hz, 2H, 5-H C_6H_4), 6.98 (d, J = 6 Hz, 4H, 4,6-H C_6H_4), 6.14/6.08 (s/s, 4H/4H, 4-H pz), 5.11 (s, 1H, 2-H C_6H_4), 2.57/2.42 (s/s, 12H/12H/, 5-H CH_3), 1.81/0.73 (s/s, 12H/12H/, 3-H CH_3), −1.15 (s, 1H, Zn−(O)H−Zn). ^{13}C NMR (100.6 MHz, acetonitrile-d_3) at 20 °C: δ 153.7/151.7/146.4/144.9 (3,5-C pz), 135.4 (1,3-C C_6H_4), 130.2 (5-C C_6H_4), 128.4 (4,6-C C_6H_4), 124.2 (2-C C_6H_4), 108.8/106.9 (4-C pz), 67.5 ($CH(pz)_2$), 15.3/10.4 (3-CH_3), 10.0/9.9 (5-CH_3). Anal. Calcd.(Found) for $C_{56}H_{69}Cl_3Zn_2N_{16}O_{13}$: C, 47.66 (45.43); H, 4.93 (4.73); N, 15.88 (15.13). MS ES(+) *m*/*z* (rel. % abund.) [assgn]: 1311 (1) $[Zn_2(\mathbf{L}_m^*)_2(OH)(ClO_4)_2]^+$, 606 (8) $[Zn_2(\mathbf{L}_m^*)_2(OH)(ClO_4)]^{2+}$, 514 (20) $[Zn(\mathbf{L}_m^*)_2]^{2+}$, 483 (92) $[\mathbf{L}_m^* + H]^+$, 371 (25) $[Zn_2(\mathbf{L}_m^*)_2(OH)]^{3+}$. HRMS: ES$^+$ (*m*/*z*): $[Zn_2(\mathbf{L}_m^*)_2(OH)(ClO_4)_2]^+$ calcd. for $[C_{56}H_{68}Cl_2Zn_2O_9N_{16}]^+$ 1311.3358; found 1311.3331.

$[Cd_2(\mu\text{-}OH)(\mu\text{-}L_m^*)_2](ClO_4)_3$, 3. **3** was prepared similarly to compound **2**, in a total of 15 mL tetrahydrofuran (THF) solution, starting from $Cd(ClO_4)_2{\cdot}6H_2O$ (0.22 g, 0.51 mmol). The reaction afforded 0.240 g (62%) of crude product. Single crystals were grown similarly as crystals of **2** and were mounted directly from the mother liquor as **3**·4CH_3CN. ^{1}H NMR (400 MHz, acetonitrile-d_3) at 20 °C: 7.66 (s, 4H, $CH(pz)_2$), 7.59 (t, J = 8.0 Hz, 2H, 5-H C_6H_4), 6.88 (d, J = 8.0 Hz, 4H, 4,6-H C_6H_4), 6.20/6.11 (s/s, 4H/4H, 4-H pz), 5.27 (s, 2H, 2-H C_6H_4), 2.55/2.46 (s/s, 12H/12H, 5-H CH_3), 2.02/1.25 (s/s, 12H/12H, 3-H CH_3), −2.43 (s, $J_{Cd-H(O)}$ = 24 Hz, 1H, Cd−(O)H−Cd). ^{13}C NMR (100.6 MHz, acetonitrile-d_3) at 20 °C: δ 154.0/152.1/146.4/145.7 (3,5-C pz, J_{C-Cd} = 4−8 Hz), 136.4 (1,3-C C_6H_4), 130.8 (5-C C_6H_4), 129.3 (4,6-C C_6H_4), 125.7 (2-C C_6H_4), 108.4/107.2 (4-C pz), 68.4 ($CH(pz)_2$), 14.6/11.4 (3-CH_3), 11.0/10.7 (5-CH_3). ^{113}Cd NMR (88.8 MHz, acetonitrile-d_3) at 20 °C: δ 79.9 (d, $J_{Cd-H(O)}$ = 29 Hz, $J_{^{111}Cd-^{113}Cd}$ = 174 Hz); proton decoupled spectra δ 79.9 (s, $J_{^{111}Cd-^{113}Cd}$ = 172 Hz). Anal. Calcd.(Found) for $C_{56}H_{69}Cl_3Cd_2N_{16}O_{13}$: C, 44.68 (44.63); H, 4.62 (4.38); N, 14.93 (14.91). MS ES(+) *m*/*z* (rel. % abund.) [assgn]: 1405 (2) $[Cd_2(\mathbf{L}_m^*)_2OH(ClO_4)_2]^+$, 653 (30) $[Cd_2(\mathbf{L}_m^*)_2OH(ClO_4)]^{2+}$, 402 (100) $[Cd_2(\mathbf{L}_m^*)_2OH]^{3+}$.

Crystallographic Studies. X-ray diffraction intensity data were collected on a Bruker SMART APEX CCD-based diffractometer (Mo Kα radiation, λ = 0.71073 Å).[14] Raw area detector data frame processing was performed with the SAINT+ and SADABS programs.[14] Final unit cell parameters were determined by least-squares refinement

dx.doi.org/10.1021/ic402073d | Inorg. Chem. 2013, 52, 11638−11649

Table 1. Selected Crystal Data and Structure Refinement for 1−3

	1·CH_3CN	1·1.5CH_3CN	2	3·4CH_3CN
formula	$C_{42}H_{40}Cl_3N_{17}O_{13}Zn_2$	$C_{43}H_{41.50}Cl_3N_{17.50}O_{13}Zn_2$	$C_{56}H_{69}Cl_3N_{16}O_{13}Zn_2$	$C_{64}H_{81}Cl_3N_{20}O_{13}Cd_2$
Fw, g mol^{-1}	1228.0	1248.53	1411.36	1669.64
cryst. syst.	triclinic	monoclinic	triclinic	triclinic
space group	$P\bar{1}$	$P2_1/m$	$P\bar{1}$	$P\bar{1}$
T, K	150(2)	150(2)	295(2)	100(2)
a, Å	14.2332(5)	10.3497(9)	11.3390(7)	10.8807(5)
b, Å	16.8433(6)	42.817(4)	12.8304(8)	13.4098(6)
c, Å	21.8771(8)	11.9166(9)	13.3422(8)	13.9681(7)
α, deg	97.669(1)	90	116.578(1)	78.558(1)
β, deg	102.779(1)	101.797(2)	99.107(1)	70.097(1)
γ, deg	94.881(1)	90	105.748(2)	85.428(1)
V, $Å^3$	5033.3(3)	5169.2(7)	1580.12(17)	1878.08(15)
Z	4	4	1	1
R_1 ($I > 2\sigma(I)$)	0.0602	0.0679	0.0503	0.0347
wR_2 ($I > 2\sigma(I)$)	0.1418	0.1516	0.0935	0.0926

of large sets of strong reflections taken from each data set. Direct methods structure solution, difference Fourier calculations, and full-matrix least-squares refinement against F^2 were performed with SHELXTL.[15] Non-hydrogen atoms were refined with anisotropic displacement parameters, the exception being disordered species. The hydrogen atoms were placed in geometrically idealized positions and included as riding atoms. Details of the data collection are given in Table 1.

Crystals of 1·CH_3CN (major product) and 1·1.5CH_3CN (minor product) were found in the same crystallization tube. Compound 1·CH_3CN crystallizes in the triclinic system. The space group $P\bar{1}$ (No. 2) was determined by the successful solution and refinement of the structure. The asymmetric unit consists of two crystallographically independent $[Zn_2(\mu\text{-OH})(\mu\text{-}\mathbf{L}_m)_2]^{3+}$ cations, six independent perchlorate anions, and two independent acetonitrile molecules. Atoms of both cations were labeled similarly, distinguished by the label suffixes A or B. The hydroxide protons of the bridging OH^- groups (O1A and O1B) could not be located by Fourier difference synthesis, and were not calculated. There are several small electron density peaks around each bridging oxygen atom, but none could be reasonably refined. These hydroxide protons may be disordered. The bridging hydroxide oxygen atom of cation "B" (O1B) showed an elongated displacement ellipsoid if refined with a single position (U_3/U_1 = 5.5) and was modeled as being split equally over two positions (O1B1 and O1B2). Positional disorder was modeled for two of the six perchlorates, using geometric restraints. Their total populations were constrained to sum to unity. Compound 1·1.5CH_3CN crystallizes in the space group $P2_1/m$ of the monoclinic system. The asymmetric unit consists of half each of two independent $[Zn_2(\mu\text{-OH})(\mu\text{-}\mathbf{L}_m)_2]^{3+}$, three independent perchlorate anions, and 1.5 independent acetonitrile molecules. Cation Zn1 is located on a crystallographic inversion center; cation Zn2 is located on a crystallographic mirror plane. The half acetonitrile lies in a mirror plane. The hydroxide group of the centrosymmetric cation is disordered across the inversion center and was refined as half-occupied. Two disordered perchlorate anions were refined with two distinct orientations with the aid of geometric restraints. The bridging hydroxide protons (O1 and O2) could not be located by Fourier difference synthesis, and were not calculated.

Compound 2 crystallizes in the triclinic system. The space group $P\bar{1}$ (No. 2) was determined by the successful solution and refinement of the structure. The asymmetric unit consists of half of one $[Zn_2(\mu\text{-OH})(\mu\text{-}\mathbf{L}_m{}^*)_2]^{3+}$ cation located on an inversion center, one disordered ClO_4^- anion on a general position (Cl2), and half of another ClO_4^- anion which is disordered across an inversion center (Cl1). Perchlorate Cl2 was refined with three disorder components. The sum of the occupancies of the three components initially refined to near unity; subsequently the occupancies were fixed near those values. Because of its location on an inversion center, only half of perchlorate Cl1 is present in the asymmetric unit. Cl1 was refined with two components, each with a fixed occupancy of 0.25. Cl−O and O−O distance restraints were used to maintain a chemically reasonable geometry for each component. Upon cooling to 100 K, there is a visible change in the diffraction pattern. Some diffraction maxima appear split, and some very weak additional peaks appear. However, because of the small size and weak diffracting power of the available crystals, the low-temperature form could not be structurally characterized.

Compound 3·4CH_3CN crystallizes in the triclinic system. The space group $P\bar{1}$ (No. 2) was confirmed by the successful solution and refinement of the structure. The asymmetric unit consists of half of one $[Cd_2(\mu\text{-OH})(\mu\text{-}\mathbf{L}_m{}^*)_2]$ cation, (formally) 1.5 perchlorate ions, and a total of two acetonitrile molecules. The complex is located on an inversion center. The bridging oxygen atom O(1) is disordered across the inversion center and was refined with half-occupancy. A good position for the hydroxide proton H(1A) was located in a difference map and refined isotropically with a d(O−H) = 0.82(2) Å distance restraint, and half-occupancy. One of the two perchlorate ions is disordered across an inversion center and is therefore only half-occupied per asymmetric unit. This ion is further disordered within the asymmetric unit, and was modeled with two 1/4-occupied components (Cl(2)/Cl(3)). The geometries of these components were restrained to be similar to that of the ordered perchlorate Cl(1). One of the two acetonitrile molecules is also disordered across an inversion center, and was modeled with three components with refined occupancies near 1/3. The total site occupancy was constrained to sum to unity.

3. RESULTS

Synthesis. The metallacycles are synthesized from the corresponding metal perchlorate hexahydrate, $M(ClO_4)_2{\cdot}6H_2O$ [M = Zn(II), Cd(II)], and the ligand ($\mathbf{L}_m$ or $\mathbf{L}_m{}^*$) in the presence of a base, triethylamine (Scheme 2). Monohydroxide bridged compounds are isolated in all cases, even in the presence of excess NEt_3. Single crystals suitable for X-ray studies were grown by vapor diffusion of Et_2O into 1 mL acetonitrile solutions. For compound 1, both 1·CH_3CN (major) and 1·1.5CH_3CN (minor) form in this procedure.

Scheme 2

$$2\,Zn(ClO_4)_2{\cdot}6\,H_2O + 2\,L_m \xrightarrow[-\,(HNEt_3)(ClO_4)]{+\,NEt_3} [Zn_2(\mu\text{-OH})(\mu\text{-}L_m)_2](ClO_4)_3 \quad (1)$$

$$2\,M(ClO_4)_2{\cdot}6\,H_2O + 2\,L_m{}^* \xrightarrow[-\,(HNEt_3)(ClO_4)]{+\,NEt_3} [M_2(\mu\text{-OH})(\mu\text{-}L_m{}^*)_2](ClO_4)_3 \quad M = Zn\ (2),\ Cd\ (3)$$

dx.doi.org/10.1021/ic402073d | Inorg. Chem. 2013, 52, 11638−11649

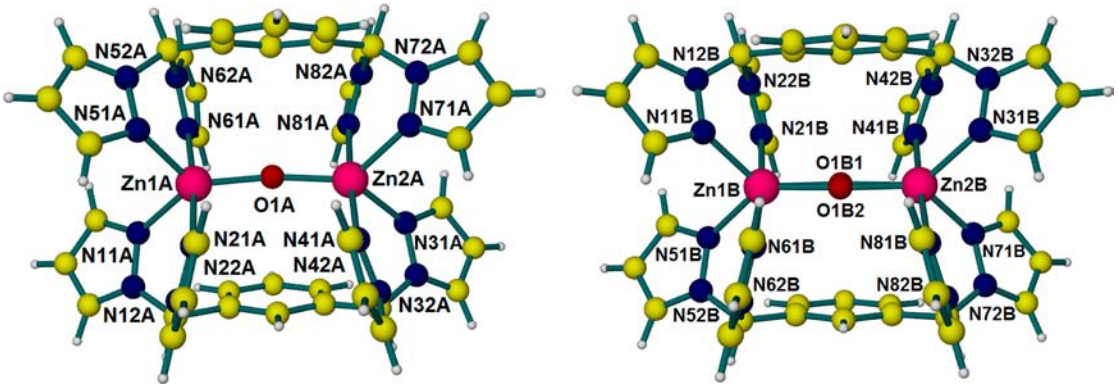

Figure 1. Structure of the two independent cationic units of $[Zn_2(\mu\text{-}OH)(\mu\text{-}\mathbf{L}_m)_2](ClO_4)_3\cdot CH_3CN$, $\mathbf{1}\cdot CH_3CN$.

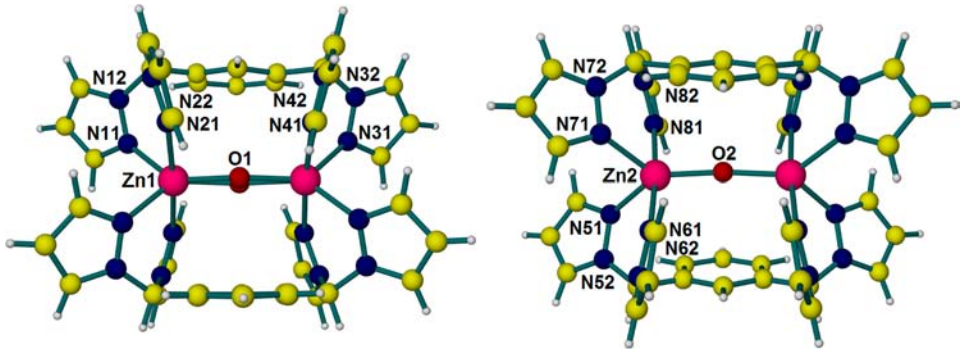

Figure 2. Structure of the two independent cationic units of $[Zn_2(\mu\text{-}OH)(\mu\text{-}\mathbf{L}_m)_2](ClO_4)_3\cdot 1.5CH_3CN$, $\mathbf{1}\cdot 1.5CH_3CN$.

Compound **2**, while crystalline, could not be completely separated from a slight impurity.

Mass Spectrometry. Positive-ion electrospray mass spectra (ESI^+-MS) of the three complexes are similar. In all spectra, clusters, such as $[M_2(\mathbf{L})_2OH(ClO_4)_2]^+$, $[M_2(\mathbf{L})_2OH(ClO_4)]^{2+}$, and $[M_2(\mathbf{L})_2OH]^{3+}$, [M = Zn(II) where **L** = $\mathbf{L}_m$ and M = Zn(II), Cd(II) where **L** = $\mathbf{L}_m$*] corresponding to the complete hydroxide bridged metallacycles are observed, demonstrating the highly stable nature of these species.

Solid State Structures. Figure 1 presents the two independent cationic units of $\mathbf{1}\cdot CH_3CN$. Similarly Figure 2 shows the two independent cationic units of compound $\mathbf{1}\cdot 1.5CH_3CN$, one rests on a plane of symmetry whereas the other resides on an inversion center. The structure and numbering scheme for the cationic unit of $\mathbf{3}\cdot 4CH_3CN$ is shown in Figure 3; the overall structure and numbering scheme of **2** are the same. Selected bond lengths and bond angles are shown in Table 2, fully labeled figures can be found in the Supporting Information, Figure S1–S3.

The structures of the three metallacycles are very similar regardless of the bis(pyrazolyl)methane ligand used (Supporting Information, Figure S4). The geometry around the metal centers in these complexes are distorted trigonal bipyramidal, as supported by the M-N bond lengths [e.g., $\mathbf{1}\cdot CH_3CN$, equatorial: Zn(1A)–N 2.085(4) Å, 2.101(5) Å; axial: Zn(1A)–N, 2.137(4) Å, 2.198(4) Å, bond angles [e.g., $\mathbf{1}\cdot CH_3CN$, axial–axial: N–Zn(1A)–N 175.12(18)°; equatorial-equatorial: N–Zn(1A)–N 98.57(18)°; N–Zn(1A)–O(1A) 128.35(18)°, 132.23(18)°, equatorial-axial: N–Zn(1A)–N 84.93(17)°, 89.51(17)°, 92.93(17)°, 86.47(17)°] and τ_5[16] values (0.63–0.73).

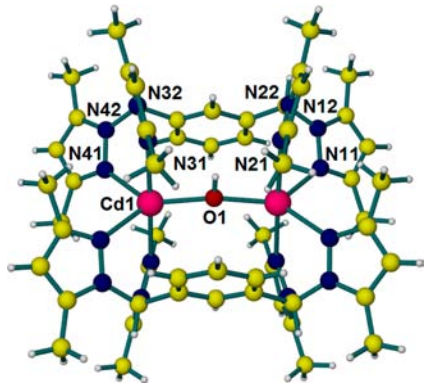

Figure 3. Structure of the cationic unit of $[Cd_2(\mu\text{-}OH)(\mu\text{-}\mathbf{L}_m{}^*)_2](ClO_4)_3\cdot 4CH_3CN$, $\mathbf{3}\cdot 4CH_3CN$. The 2-fold disorder of the bridging hydroxide is removed for clarity.

The predicted values for the M-O(H) distances were calculated by summing the ionic radius of each metal center with the ionic radius of the hydroxide ion.[17] The calculated values are in good agreement with the measured M-O(H) distances. The Zn–O(H) distances for the $\mathbf{L}_m$ compound are slightly shorter than predicted, while the bulkier ligand $\mathbf{L}_m$* compounds have longer bond lengths than predicted by 0.071–0.102 Å. These deviations indicate that the M-O(H) distances are influenced by the steric properties of the bis(pyrazolyl)-methane ligand. The M-O-M angles, 163.6(3)/164.8° for $\mathbf{1}\cdot CH_3CN$, 162.4(7)/167.2(5)° for $\mathbf{1}\cdot 1.5CH_3CN$, 180° for **2**, and 161.36(14)° for $\mathbf{3}\cdot 4CH_3CN$, are very large for a bridging hydroxide (commonly between 90 and 120°).[5a,c] The ligands $\mathbf{L}_m$ and $\mathbf{L}_m$* support the metallacyclic structures and influence

dx.doi.org/10.1021/ic402073d | Inorg. Chem. 2013, 52, 11638–11649

Table 2. Selected Bond Lengths and Bond Angles for $[Zn_2(\mu\text{-}OH)(\mu\text{-}L_m)_2](ClO_4)_3\cdot CH_3CN$, 1·$CH_3CN$; $[Zn_2(\mu\text{-}OH)(\mu\text{-}L_m)_2](ClO_4)_3\cdot 1.5CH_3CN$, 1·1.5$CH_3CN$; $[Zn_2(\mu\text{-}OH)(\mu\text{-}L_m{*})_2](ClO_4)_3$, 2; $[Cd_2(\mu\text{-}OH)(\mu\text{-}L_m{*})_2](ClO_4)_3\cdot 4CH_3CN$, 3·4$CH_3CN$

	1·CH_3CN	1·1.5CH_3CN	2	3·4CH_3CN
temp, K	150(2)	150(2)	295(2)	100(2)
metal centers	Zn(1A)−Zn(2A) Zn(1B)−Zn(2B)	Zn(1)−Zn(1) Zn(2)−Zn(2)	Zn(1)−Zn(1)	Cd(1)−Cd(1)
M-O-M angle, deg	163.6(3) 164.8[a]	162.4(7) 167.2(5)	180	161.36(14)
M-O length, Å	1.961(4)/1.934(4) 1.960/1.967[b]	1.939[b] 1.9737(13)	2.0407(6)	2.1505[b]
predicted M-O length, Å[c]	2.0	2.0	2.0	2.19
average M-N length, Å	2.130/2.133 2.143/2.137	2.139 2.134	2.135	2.337
M···M distance, Å	3.855 3.889	3.831 3.923	4.0814	4.244
τ_5	0.72/0.73 0.63/0.68	0.65 0.65	0.72	0.72

[a]Average bond angle, because of disorder. [b]Average bond length, because of disorder. [c]Shannon Radii, ref 17.

the M···M nonbonding distance, resulting in large M-O-M angles.

Ambient Temperature NMR Studies. The ambient temperature ^1H and ^{13}C NMR spectra of **1**−**3** revealed that the dinuclear structure remains intact in acetonitrile solution, as reported previously with the fluoride bridged metallacycles, $[Zn_2(\mu\text{-}F)(\mu\text{-}L)_2](BF_4)_3$ (L = L_m or L_m*).[6] The presence of a highly symmetric species is indicated by the ^1H NMR spectra in Figure 4 of $[Zn_2(\mu\text{-}OH)(\mu\text{-}L_m)_2](ClO_4)_3$, **1** (a) and $[Cd_2(\mu\text{-}OH)(\mu\text{-}L_m{*})_2](ClO_4)_3$, **3** (b), which show three resonances for the ligand 1,3-substituted phenylene spacer (e.g., **1**: 7.56, 6.63, and 4.75 ppm) and one for the methine hydrogens (e.g., **1**: 8.15 ppm). For the pyrazolyl-ring hydrogen atoms, two distinct sets of equal intensity resonances are observed. The 4(*b*)-pyrazolyl hydrogens of **1** can be found at 6.52 and 6.42 ppm, the 5(*c*)-pyrazolyl hydrogens are at 8.40 and 8.19 ppm, while the 3(*a*)-pyrazolyl hydrogens are at 7.48 and 6.64 ppm. The resonances for the *c**- and *a**-methyl groups are at 2.57, 2.42, 1.81, and 0.73 ppm for **2**, and at 2.55, 2.46, 2.02, and 1.25 ppm for **3**, respectively. For all compounds, one pyrazolyl resonance is highly shielded. These hydrogens correspond to one of the axial pyrazolyl hydrogens or methyl groups that are pointing toward the phenylene spacers (Figure 5). This assignment makes the 3(*a*)/*a**- and 5(*c*)/*c**-positions distinguishable by ^1H NMR spectroscopy.

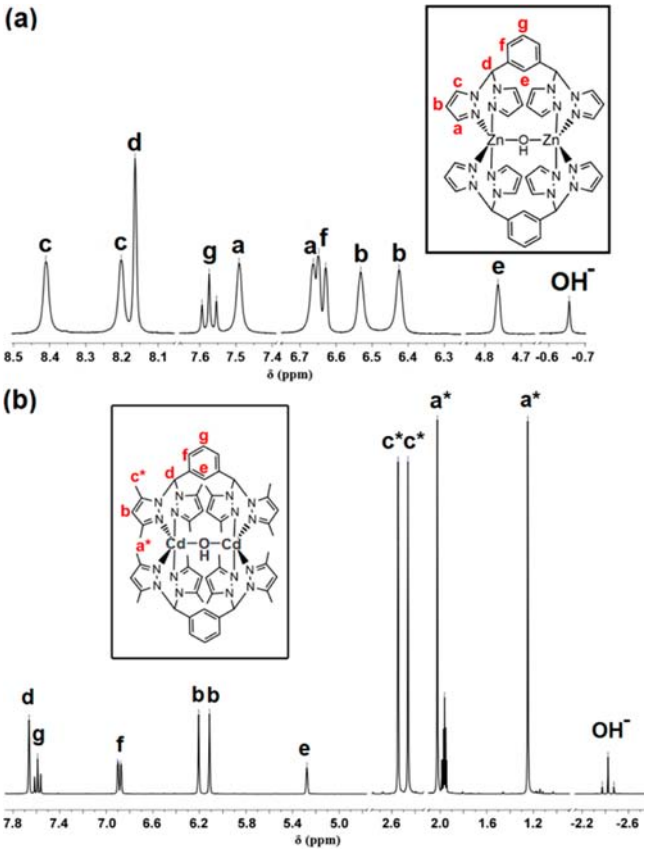

Figure 4. Ambient temperature ^1H NMR spectra of $[Zn_2(\mu\text{-}OH)(\mu\text{-}L_m)_2](ClO_4)_3$, **1**, (a) and $[Cd_2(\mu\text{-}OH)(\mu\text{-}L_m{*})_2](ClO_4)_3$, **3** (b).

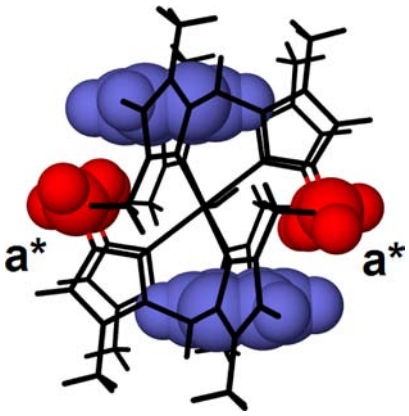

Figure 5. Shielded *a** methyl groups in the structure of $[Cd_2(\mu\text{-}OH)(\mu\text{-}L_m{*})_2](ClO_4)_3$, **3** (red = methyl group; blue = phenylene spacer).

The resonances corresponding to the bridging OH^- are located at −0.66 ppm (**1**), −1.15 ppm (**2**), and −2.43 ppm (**3**). Similar assignments were made in Co(III) dimers by Bosnich et al., where the hydroxide resonance was found in the range 0.57 to −2.42 ppm in CD_3CN solution.[18]

The retention of the solid state structure in solution was also confirmed by measuring the diffusion coefficient for complex **1** by pulsed field-gradient spin−echo NMR (PFGSE NMR).[19]

The hydrodynamic radius based on the diffusion coefficient from this experiment is 8.93 Å, similar to the maximum radius for the dinuclear unit, calculated from the crystal structure of **1**, 8.20 Å.

At room temperature, the ^{13}C NMR spectrum of **1** shows that the pyrazolyl resonances are very broad and the 5(*c*), 144.6 ppm, as well as the 4(*b*), 108.4 ppm, pyrazolyl resonances coalesced. At −40 °C two sharp resonances are observed for each pyrazolyl hydrogen: 5(*c*) 143.7/142.9 ppm, 3(*a*) 137.00/135.22 ppm, 4(*b*) 107.14/107.00 ppm (Supporting Information, Figure S5).

The ^{13}C and ^{113}Cd NMR spectra of **3** demonstrate several interesting features. The ^{13}C NMR spectrum shows coupling of the 3(*a*)- and 5(*c*)-pyrazolyl carbons with the cadmium(II) centers, J_{C-Cd} = 4−8 Hz, while in the ^{113}Cd NMR spectrum the coupling of the cadmium(II) centers to the bridging hydroxide hydrogen can be observed (Figure 6). Without proton decoupling a doublet is observed at 79.9 ppm; the coupling constant, $J_{Cd-H(O)}$ = 29 Hz, is the same as the coupling constant observed for the cadmium(II) satellites in the ^{1}H NMR spectrum, $J_{(O)H-Cd}$ = 32 Hz (Figure 4b). The proton decoupled ^{113}Cd NMR spectra of **3** shows only a singlet. Particularly interesting and important features are the $^{111/113}Cd$ satellites in both coupled and decoupled spectra ($J^{111}_{Cd-}{}^{113}_{Cd}$ = 173 Hz, both of these spin 1/2 isotopes are about 13% abundant).

Variable-Temperature ^{1}H NMR Studies. The broad or coalesced pyrazolyl hydrogen resonances observed at ambient temperature in the ^{1}H and ^{13}C NMR spectra of **1** are indicative of a dynamic process in solution. The variable-temperature ^{1}H NMR spectra of **1** over the liquid range of CD_3CN, Figure 7,

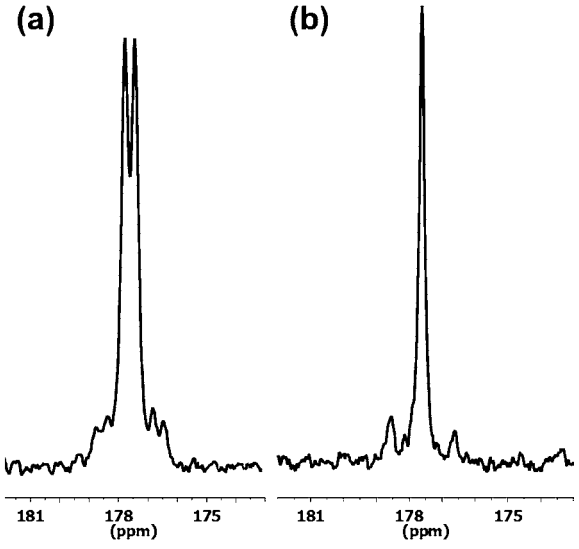

Figure 6. ^{113}Cd NMR of $[Cd_2(\mu\text{-OH})(\mu\text{-}\mathbf{L}_m{}^*)_2](ClO_4)_3$, **3**: (a) proton coupled, (b) proton decoupled.

show major changes, confirming that the complex is indeed dynamic on the NMR time scale in solution. A trace amount of H_2O, present in the deuterated solvent, was observed in all spectra. The relative amount of water in these experiments, an important issue (vide infra), was defined as the integral of the H_2O resonance divided by the integral of the *e* resonance at 25 °C, a ratio that is equal to 5 for the data in Figure 7. Under similar conditions, the resonances in the ^{1}H NMR spectra of compounds **2** and **3** remain sharp up to 75 °C, indicating the lack of a similar dynamic process in these complexes.

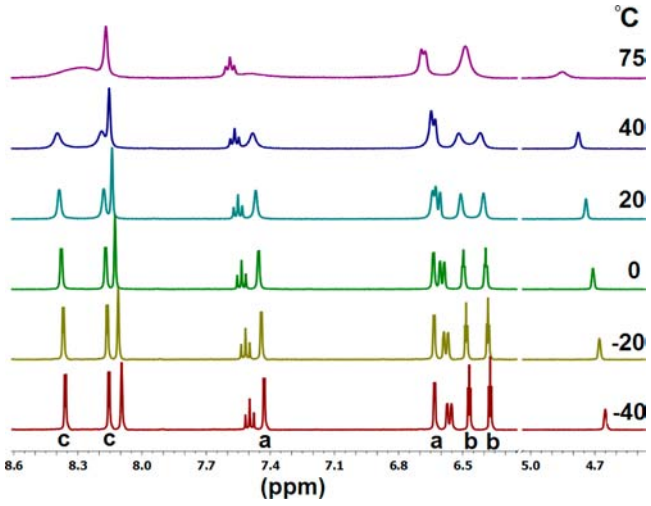

Figure 7. Variable-temperature ^{1}H NMR spectra of $[Zn_2(\mu\text{-OH})(\mu\text{-}\mathbf{L}_m)_2](ClO_4)_3$ (**1**) from −40 to 75 °C in CD_3CN.

For **1**, the pyrazolyl resonances assigned to the 3(*a*)/5(*c*) positions were resolved as doublets and the 4(*b*) positions as triplets upon cooling the sample to −40 °C. At high temperature (75 °C), the resonances corresponding to the nonequivalent pyrazolyl rings average, only one set of 4(*b*) and 5(*c*) and two very broad 3(*a*) resonances could be observed. The limiting high temperature spectrum could not be reached as the boiling point of CD_3CN is 81.6 °C.

The rate constant (k_{pz}) for the exchanging pyrazolyl resonances was calculated two different ways.[20]

(a) From the experimental data measuring the broadening in excess of the natural line width ($W_{1/2}$) before coalescence via eq 1 (Figure 8, left);

$$k = \pi \cdot W_{1/2} \tag{1}$$

(b) By simulation of the exchanging resonances using the program DNMR as implemented in Spinworks[21] (Figure 8, right). We chose to simulate the exchange of the 5(*c*)-pyrazolyl hydrogen atoms.

The Gibbs energy of activation, $\Delta G_{pz}{}^{\ddagger}$, was calculated by applying the modified Eyring equation, eq 2, to the rate constants, where *R* is the universal gas constant and *T* is the temperature. The two methods (a, b) resulted in identical $\Delta G_{pz}{}^{\ddagger}$ values, 15.2(±0.2) kcal/mol at 25 °C.

$$\Delta G^{\ddagger} = RT\left(23.759 + \ln\frac{T}{k}\right) \tag{2}$$

The enthalpy of activation, $\Delta H_{pz}{}^{\ddagger}$, 6.6 (±0.1) kcal/mol, and entropy of activation, $\Delta S_{pz}{}^{\ddagger}$, −28.8 (±0.4) cal/mol·K, were calculated from the Eyring plot (Figure 9). More than half of the value for $\Delta G_{pz}{}^{\ddagger}$ comes from the $T\cdot\Delta S_{pz}{}^{\ddagger}$ term (when $\Delta G_{pz}{}^{\ddagger} = \Delta H_{pz}{}^{\ddagger} - T\cdot\Delta S_{pz}{}^{\ddagger}$). The negative entropy value indicates that the transition state is highly organized.[22]

Impact of Water Concentration on the VT-NMR Spectra. Similar VT-NMR studies were carried out on 5 different samples of **1**, where the concentration of the zinc(II) complex was maintained constant (3 mg in 800 μL CD_3CN), but the concentration of H_2O in the CD_3CN was varied. At 25 °C the linewidths of the phenylene resonances are not affected significantly by the concentration of H_2O in the sample, but the pyrazolyl resonances undergo severe line width broadening in the presence of increased amounts of H_2O. As a consequence,

dx.doi.org/10.1021/ic402073d | *Inorg. Chem.* 2013, 52, 11638−11649

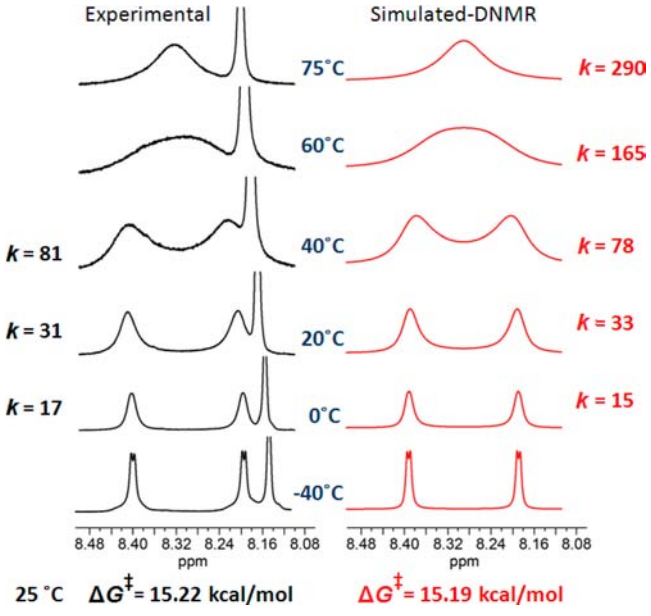

Figure 8. 5(*c*)-Pyrazolyl proton resonances of $[Zn_2(\mu\text{-OH})(\mu\text{-L}_m)_2](ClO_4)$ (**1**). Left: experimental spectra, showing the rate constants at different temperatures and the calculated $\Delta G^{\ddagger}$ in black as determined using method (a). Right: simulated ^{1}H NMR spectra, corresponding rate constants, and calculated $\Delta G^{\ddagger}$ shown in red using method (b).

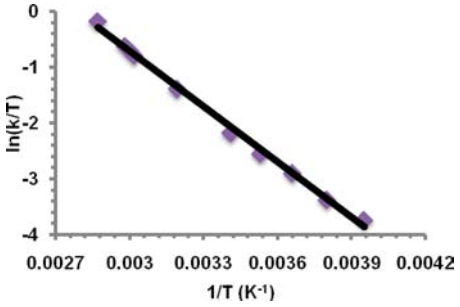

Figure 9. Eyring plot based on k_{pz} values from the simulation of the 5(*c*)-pyrazolyl resonances of $[Zn_2(\mu\text{-OH})(\mu\text{-L}_m)_2](ClO_4)_3$ at different temperatures, where the slope is $-\Delta H^{\ddagger}/R$; and the intercept is $\Delta S^{\ddagger}/R$ + 23.759. The data points were fitted to $y = -3324.5x + 9.2673$ (R^2 = 0.9968).

the $\Delta G^{\ddagger}$ for the pyrazolyl exchange is dependent on the concentration of trace amounts of water in the sample (Figure 10). Since the absolute concentration of the water is unknown, we express it as the ratio of the integral of the H_2O resonance divided by the integral of the $\mathbf{L}_m$ ligand *e* resonance at 25 °C. Drying the CD_3CN by vacuum distillation from P_2O_5 yielded the lowest ratio of 0.6.

The plot of $\Delta G_{pz}^{\ddagger}$ vs the relative water concentration reveals a linear relationship (Figure 11). This dependence of $\Delta G_{pz}^{\ddagger}$ on the water concentration in the sample indicates that water acts to accelerate the process. The $\Delta H_{pz}^{\ddagger}$ and $\Delta S_{pz}^{\ddagger}$ were found by creating the Eyring plot from the variable temperature data for each sample; these activation parameters are shown in Table 3.

Saturation Transfer NMR Experiments. Samples of complexes **1**−**3** in CD_3CN were subject to two different saturation transfer experiments. We first targeted the exchange of the axial and equatorial 3(*a*)-pyrazolyl hydrogens in **1** [$c(H_2O)_{rel}$ = 5], the same process studied in the VT-NMR

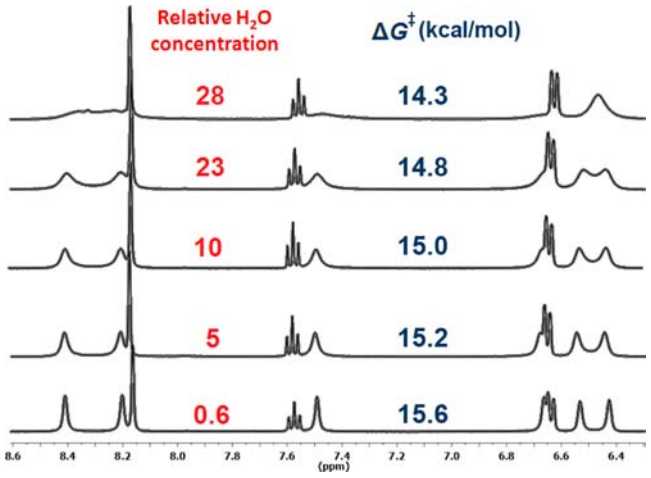

Figure 10. Fragment of the ^{1}H NMR spectra of five different samples of $[Zn_2(\mu\text{-OH})(\mu\text{-L}_m)_2](ClO_4)_3$ (**1**) in CD_3CN at 25 °C that differ only in the relative H_2O concentration.

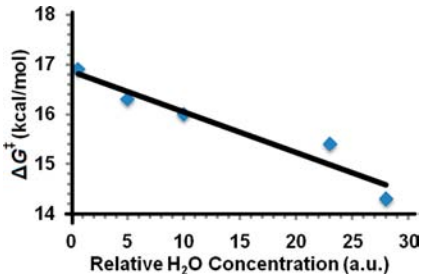

Figure 11. Relationship between the relative H_2O concentration (five samples) and $\Delta G_{pz}^{\ddagger}$ for $[Zn_2(\mu\text{-OH})(\mu\text{-L}_m)_2](ClO_4)_3$ (**1**) at 25 °C. The data points were fitted to $y = -0.0811x + 16.86$ (R^2 = 0.9278).

Table 3. Activation Parameters at 25°C Calculated Based on Eyring Plot of Simulated k_{pz} Values for the Pyrazolyl Exchange in $[Zn_2(\mu\text{-OH})(\mu\text{-L}_m)_2](ClO_4)_3$ (1) at Five Different H_2O Concentrations

sample	$c(H_2O)_{rel}$[a]	$\Delta H_{pz}^{\ddagger}$ (kcal/mol)	$\Delta S_{pz}^{\ddagger}$ (cal/mol·K)	$\Delta G_{pz}^{\ddagger}$ (kcal/mol)	T_c[b] (°C)
1	28	5.6 (±0.2)	−29.5 (±0.4)	14.3 (±0.3)	25
2	23	6.1 (±0.1)	−29.5 (±0.4)	14.8 (±0.2)	45
3	10	6.4 (±0.1)	−29.0(±0.3)	15.0 (±0.2)	56
4	5	6.6 (±0.1)	−28.8 (±0.4)	15.2 (±0.2)	62
5	0.6	7.1 (±1.2)	−28.7 (±4.4)	15.6 (±2.5)	70

[a] $c(H_2O)_{rel}$ = integral of H_2O resonance divided by integral of *e* resonance at 25°C. [b] Coalescence temperatures of the 5(*c*)-resonances.

experiments. In the second experiment we studied the exchange of the H_2O hydrogens (from solvent) with the hydrogen of the bridging hydroxide group in all three complexes.

During the saturation transfer experiments we follow pairs of exchanging resonances, for example, in the first experiment the axial and equatorial 3(*a*)-pyrazolyl resonances of **1**. Saturation of one of the exchanging resonances results in a decrease in the intensity of the other resonance. This decrease in intensity is a function of irradiation time. In the experiments, the irradiation time is increased in 0.25 s intervals until the intensity of the

dx.doi.org/10.1021/ic402073d | Inorg. Chem. 2013, 52, 11638−11649

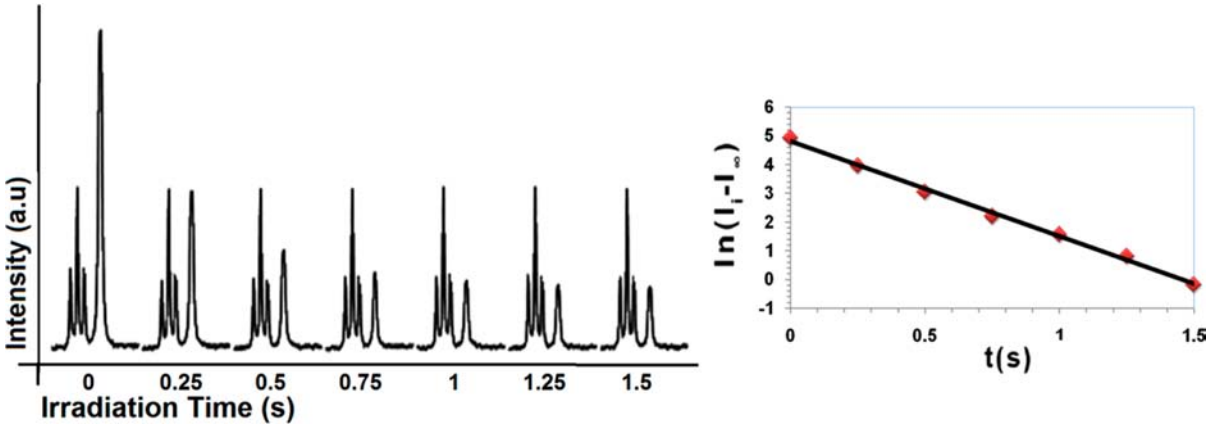

Figure 12. Saturation transfer experiment targeting the axial−equatorial pyrazolyl exchange in $[Zn_2(\mu\text{-}OH)(\mu\text{-}L_m)_2](ClO_4)_3$ (**1**) at −40 °C. Left: decrease of one of the 3(*a*)-pz resonances as a function of the irradiation time of the other 3(*a*)-pz resonance. As the height of the pyrazolyl resonance decreases upon increased saturation times, the height of the neighboring phenylene triplet (resonance *g*) remains constant, as it is not part of the exchange process. Right: linear plot of the natural logarithm of the 3(*a*)-pz resonance intensities vs irradiation time. Data fitted to $y = -3.3055x + 4.8098$ ($R^2 = 0.9965$).

second resonance remains constant. The natural logarithm of this decrease in intensity is proportional to the rate constant (k).

Following literature methods[23] we have plotted the values of $\ln(I_i - I_\infty)$ against the irradiation time (t) as seen in Figure 12, where I_i is the residual intensity of the exchanging resonance after intermediate amounts of irradiation times and I_∞ is the residual intensity of the exchanging resonance after complete saturation. The slope of this straight line gives $-(1/\tau_{1a})$, where τ_{1a} is the overall lifetime of the process, which includes the spin−lattice relaxation time (T_{1a}) and the lifetime of the equatorial 3(*a*)-pz proton in the axial 3(*a*)-pz site (τ_a). A standard inversion recovery experiment results in values of T_{1a}. By substitution of the known values into eq 3, $1/\tau_a$ was calculated, which is equal to k (eq 4) if the equilibrium is first order. The $\Delta G^{\ddagger}$ was calculated by applying the modified Eyring equation to k.

$$\frac{1}{\tau_{1a}} = \frac{1}{\tau_a} + \frac{1}{T_{1a}} \tag{3}$$

$$k = \frac{1}{\tau_a} \tag{4}$$

We carried out the saturation transfer experiments targeting the pyrazolyl exchange at −40 °C, to study sharp and clearly separated resonances (Figure 12). The resulting $\Delta G_{pz}^{\ddagger}$ at −40 °C for the pyrazolyl exchange, 13.1(±0.2) kcal/mol, is in very good agreement with the one calculated from the VT-NMR experiment, $\Delta G_{pz}^{\ddagger}$ = 13.2(±0.2) kcal/mol at −40 °C for the same sample.

The second spin saturation experiment demonstrates the exchange of the hydrogens between H_2O, present in the solvent, and the bridging hydroxide (Figure 13). Upon complete saturation of the H_2O resonance, the bridging hydroxide resonance almost disappears at 25 °C.

The $\Delta G_{OH}^{\ddagger}$ calculated from the saturation transfer experiment for the exchange of hydrogen from water and the bridging hydroxide is 16.8(±0.2) kcal/mol at 25 °C. For comparison, $\Delta G_{pz}^{\ddagger}$ is 15.2(±0.2) kcal/mol at 25 °C from the VT-NMR data shown in Figure 8. To directly compare $\Delta G_{OH}^{\ddagger}$ and $\Delta G_{pz}^{\ddagger}$ from saturation transfer experiments, the experiment performed at 25 °C was repeated at −40 °C, resulting in $\Delta G_{OH}^{\ddagger}$ = 14.4(±0.2) kcal/mol (Figure 14). This value for $\Delta G_{OH}^{\ddagger}$ is larger by 1.3 kcal/mol compared to $\Delta G_{pz}^{\ddagger}$ = 13.1(±0.2) kcal/mol, as determined above.

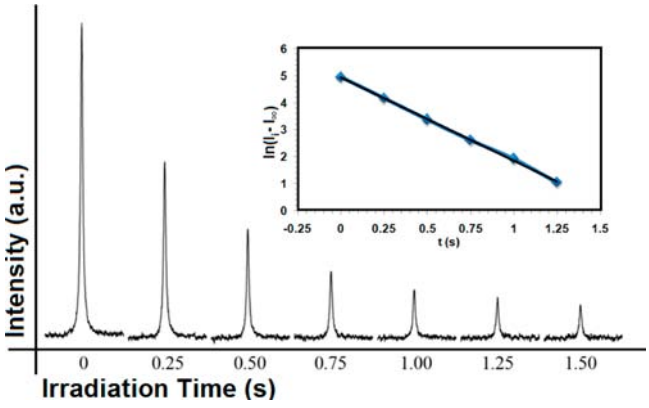

Figure 13. Saturation transfer experiment targeting the exchange of hydrogen between H_2O and OH^- for $[Zn_2(\mu\text{-}OH)(\mu\text{-}L_m)_2](ClO_4)_3$ (**1**) at 25 °C. The intensity of the bridging OH^- resonance decreases as a function of irradiation time at the H_2O site. Inset: linear plot of the natural logarithm of the OH^- resonance intensity vs the irradiation time. Data fitted to $y = -3.0839x + 4.944$ ($R^2 = 0.9994$).

Room temperature pyrazolyl saturation transfer experiments for **2** and **3** show that the pyrazolyl rings are not exchanging, but the H_2O−OH^- hydrogen exchange can be followed. The rate constants (**2**: $k_{OH} = 0.70\ s^{-1}$; **3**: $k_{OH} = 0.47\ s^{-1}$) at 25 °C show that the hydrogen exchange is slower for $\mathbf{L}_m$* compounds than for $\mathbf{L}_m$ compounds (**1**: $k_{OH} = 2.85\ s^{-1}$). Consequently $\Delta G_{OH}^{\ddagger}$ increases by 1.0−1.3 kcal/mol (**2**, $\Delta G_{OH}^{\ddagger}$ = 17.7(±0.2) kcal/mol; **3**, $\Delta G_{OH}^{\ddagger}$ = 17.9(±0.2) kcal/mol vs. **1**, $\Delta G_{OH}^{\ddagger}$ = 16.8(±0.2) kcal/mol).

5. DISCUSSION

We successfully isolated three diamagnetic monohydroxide bridged Zn(II) and Cd(II) complexes of the type $[M_2(\mu\text{-}OH)(\mu\text{-}L)_2](ClO_4)_3$, **L** = $\mathbf{L}_m$ or $\mathbf{L}_m$*. Coordination of the four pyrazolyl nitrogens from two different ligands oriented in a *syn* conformation [both bis(pyrazolyl)methane units on the same side of the linking phenylene ring] to two metal centers with a hydroxide directly connecting the metal centers results in the

dx.doi.org/10.1021/ic402073d | *Inorg. Chem.* 2013, 52, 11638−11649

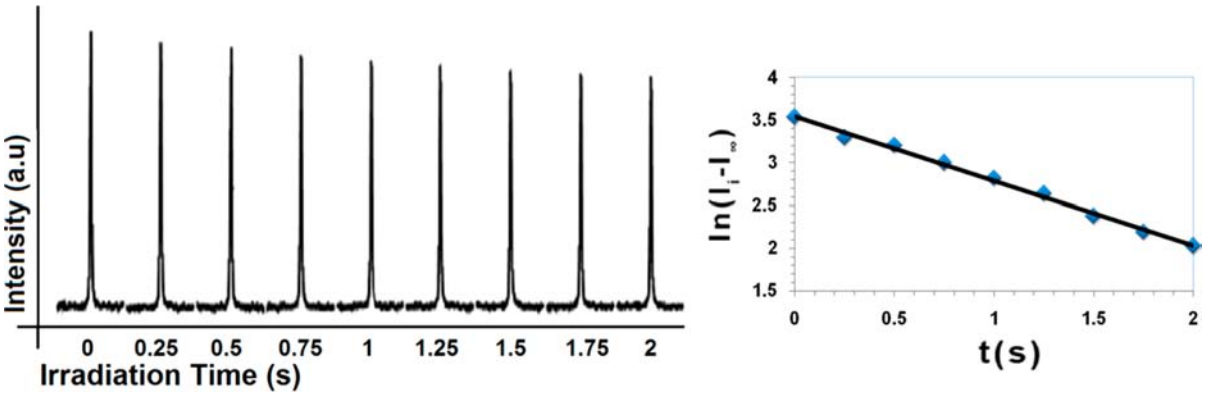

Figure 14. Saturation transfer experiment targeting the exchange of the hydrogens from H_2O and OH^- in $[Zn_2(\mu\text{-}OH)(\mu\text{-}L_m)_2](ClO_4)_3$ (**1**) at −40 °C. Left: decrease of the OH^- resonance as a function of irradiation time at the H_2O site. Right: linear plot of the natural logarithm of the OH^- resonance intensities vs irradiation time. Data fitted to $y = -0.7581x + 3.5429$ ($R^2 = 0.9952$).

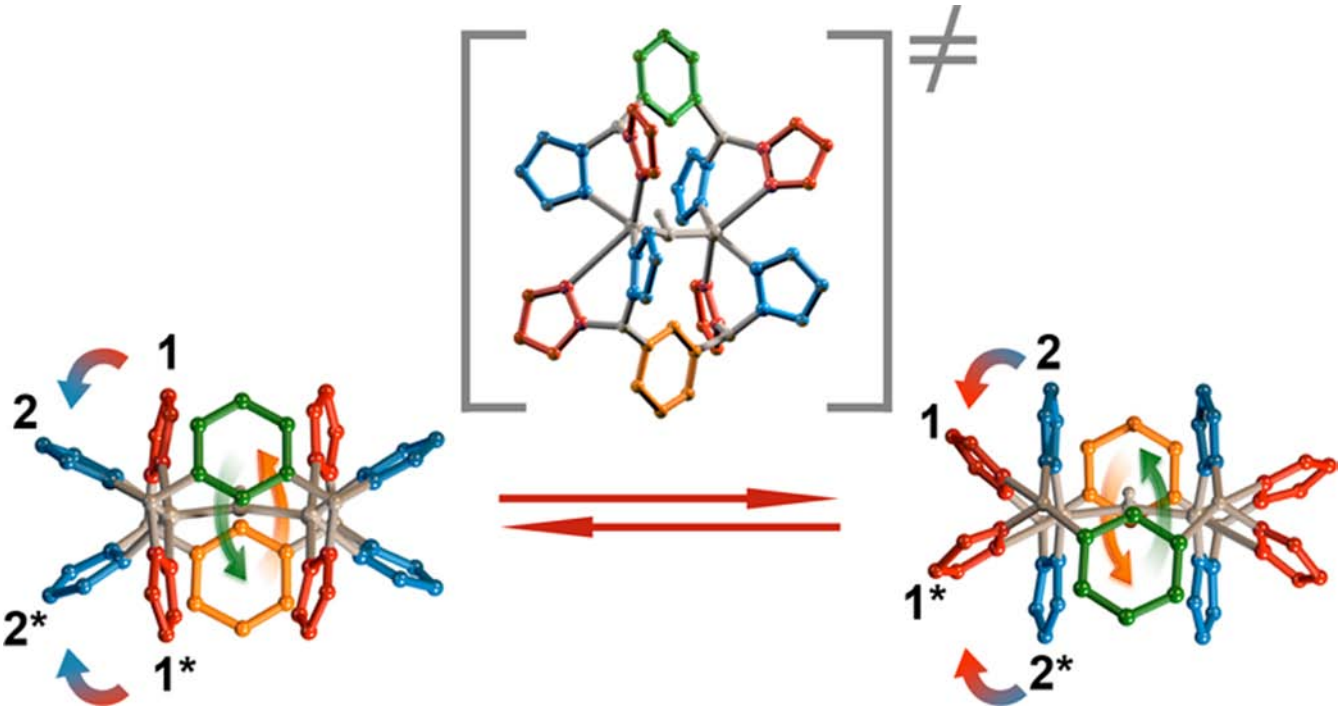

Figure 15. "Columbia Twist and Flip" involving the concerted double Berry pseudorotation of the pyrazolyl rings and the accompanied 180° flip of the phenylene linkers for $[Zn_2(\mu\text{-}OH)(\mu\text{-}L_m)_2](ClO_4)_3$ (**1**). The 1 and 1* pz rings exchange with the 2 and 2* pz rings through a square pyramidal intermediate. The proposed intermediate (in brackets) is rotated 90° to show the approximate square pyramidal geometry around copper(II). Phenylene spacer top = green, bottom = orange; left side: axial pyrazolyl rings = red, equatorial pyrazolyl rings = blue, right side: axial pyrazolyl rings = blue, equatorial pyrazolyl rings = red. (See also the attached WEO animation in mpg format).

monobridged metallacyclic structures, with metal centers in distorted trigonal bipyramidal geometry.

These complexes were shown to retain this structure in solution and in gas phase according to ^1H, ^{13}C, and ^{113}Cd NMR and positive-ion ESI^+-MS studies, respectively. For example, the observation in the ^1H NMR spectra of one type of phenylene and methine resonances and two types of pyrazolyl signals (two distinct sets of resonances for each type of pyrazolyl ring) are in complete agreement with the solid state structure, where the pyrazolyl rings are in the equatorial and axial plane of the trigonal bipyramidal arrangement around the metal centers. The bridging hydroxide proton resonances are characteristically located in the interval −0.66 to −2.43 ppm,[18] and in the case of **3** shows coupling to cadmium(II).

VT-NMR experiments often give important structural details about molecular motion in solution.[24] In this work, complex **1** was shown to be dynamic in solution by this method. Two sets of broad pyrazolyl resonances for each type of ring hydrogen can be observed at room temperature, which broaden and/or coalesce at higher temperatures. This behavior corresponds to the exchange of the axial and equatorial pyrazolyl rings. The activation parameters derived from the Eyring plot at different temperatures are $\Delta G_{pz}^{\ddagger} = 15.2(\pm0.2)$ kcal/mol, $\Delta H_{pz}^{\ddagger} = 6.6(\pm0.1)$ kcal/mol, and $\Delta S_{pz}^{\ddagger} = -28.8(\pm0.4)$ cal/mol·K at 25 °C. Most notably, this large negative $\Delta S_{pz}^{\ddagger}$ is unusual for most fluxional processes[24] and is indicative of a highly organized transition state.[22]

Saturation transfer experiments were also used to study the dynamics of **1**. Saturation of one pyrazolyl resonance of the

dx.doi.org/10.1021/ic402073d | Inorg. Chem. 2013, 52, 11638−11649

exchanging pairs results in a decrease in the intensity of the second corresponding pyrazolyl resonance. This experiment was best carried out at −40 °C to avoid resonance overlap and to carry out the intensity measurements on narrow resonances, yielding $\Delta G_{pz}^{\ddagger}$ = 13.1(±0.2) kcal/mol, a value comparable to $\Delta G_{pz}^{\ddagger}$ from VT-NMR experiment of 13.2(±0.2) kcal/mol at −40 °C. These results show that this experiment is advantageous for the study of mutual-site exchange kinetics, especially when the coalescence temperature exceeds the boiling point of the solvent or the limiting low temperature spectra cannot be reached, basically allowing the analyses of k in the range ∼10^{-3} to 10^{2} s^{-1}.

The most plausible mechanism for this relatively low barrier dynamic process, which exchanges the axial and equatorial pyrazolyl rings in the trigonal bipyramidal arrangement around the metal centers, involves the Berry pseudorotation at *both metal sites* using the bridging oxygen atom as the pivot ligand, coupled with the rotation of the ligand's phenylene spacer by 180° (ring flip) along the $C_{methine}$-C_{Ph} bond (Figure 15, see also WEO animation). This movement results in the exchange of the axial (left, 1, 1*) and equatorial (left, 2, 2*) pyrazolyl rings through an approximately square pyramidal transition state at each metal, where the square bases are occupied by the interchanging pyrazolyl groups. The two originally equatorial ligands move to the axial sites, reestablishing the trigonal bipyramidal geometry.[25] The main advantages of this mechanism are that no bond cleavage is necessary and relatively small bond angle changes are required around the central zinc(II) ions, which support a relatively low $\Delta H_{pz}^{\ddagger}$. The transition state involves a distorted square pyramidal arrangement around each zinc(II), where the four pyrazolyl rings are approximately in the same plane, explaining the relatively large negative $\Delta S_{pz}^{\ddagger}$. Following the precedence of Chisholm et al., describing the mechanism of a rearrangement for a very different dinuclear dynamic system ("Bloomington Shuffle"),[26] we have termed this new rearrangement process the "*Columbia Twist and Flip*."

The energy barrier for the Berry pseudorotation in PF_5 is ∼3.1 kcal/mol.[27] The Columbia Twist and Flip is energetically more demanding than the unhindered rotation of fluorine atoms, because of the size of the pyrazolyl rings and the rigidity of the dinuclear unit, leading to a barrier of 15.2(±0.2) kcal/mol. A mononuclear case similar to the dynamic behavior of $[Zn_2(\mu\text{-OH})(\mu\text{-}\mathbf{L}_m)_2](ClO_4)_3$ (**1**) was studied by Moore et al., $[ZnCl(\mathbf{L}_c)]ClO_4$ where L_c = 1,4,8,11-tetramethyl-1,4,8,11-tetraazacyclotetradecane.[28] The zinc(II) center is five coordinate with four nitrogen donors and a chloride. In solution, as revealed by the ^{13}C NMR, the geometry is trigonal bipyramidal. Similarly to $[Zn_2(\mu\text{-OH})(\mu\text{-}\mathbf{L}_m)_2](ClO_4)_3$, two ligand nitrogen atoms occupy axial and two equatorial sites. The compound undergoes Berry pseudorotation to equilibrate the nonequivalent sites with activation parameters, $\Delta G^{\ddagger}$ = 13.0(±1.0) kcal/mol, $\Delta H^{\ddagger}$ = 14.1(±0.7) kcal/mol, and $\Delta S^{\ddagger}$ = 3.6 (±2.9) cal/mol·K at 25 °C. The contribution to $\Delta G^{\ddagger}$ from the $\Delta S^{\ddagger}$ term for this mononuclear complex is low, indicating that in the case of **1** the large negative $\Delta S^{\ddagger}$ contribution is a result of the dinuclear structure and the rigidity of the system.

A somewhat similar dynamic process in a dinuclear system has been reported by Gardiner et al.[29] for four-coordinate silver(I) metallacycles, such as $[Ag_2(\mu\text{-}\mathbf{L}_l)_2](BF_4)_2$ ($\mathbf{L}_l$ = α,α,α′,α′-tetra(pyrazolyl)lutidine). In this system, the data indicate that monomeric complexes are present in solution and are responsible for the dynamic behavior. While the results of the PFGSE NMR in their case supports this hypothesis, for compound **1** the calculated hydrodynamic radius based on the diffusion coefficient supports the dinuclear structure in solution, as do the observation of $[Zn_2(\mathbf{L}_m)_2(OH)(ClO_4)_2]^{+}$ and $[Zn_2(\mathbf{L}_m)_2(OH)(ClO_4)]^{2+}$ peaks in the mass spectrometric measurements. In addition, the $^{113}Cd/^{111}Cd$ coupling in **3** (Figure 6) definitively shows this sterically more hindered complex does not rapidly dissociate into monomers in solution.

The spectra of compounds **2** and **3** do not change at different temperatures. The space filling models of $[Zn_2(\mu\text{-OH})(\mu\text{-}\mathbf{L}_m)_2](ClO_4)_3$ and $[Zn_2(\mu\text{-OH})(\mu\text{-}\mathbf{L}_m{*})_2](ClO_4)_3$, Figure 16,

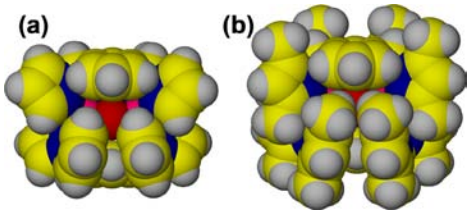

Figure 16. Space-filling representation of $[Zn_2(\mu\text{-OH})(\mu\text{-}\mathbf{L}_m)_2](ClO_4)_3$ (a) and $[Zn_2(\mu\text{-OH})(\mu\text{-}\mathbf{L}_m{*})_2](ClO_4)_3$ (b).

illustrate that the substitution of the pyrazolyl rings in the 3(*a*) and 5(*c*) positions causes steric crowding. The methyl groups sterically restrict the rotation of the pyrazolyl rings; a square pyramidal transition state is very unlikely in this case. Similar tuning of the molecular motion is observed in molecular rotors, where substitution of bulky groups on the stator or rotator hinders the motion.[2−4]

We have also shown that the pseudorotation is influenced by the concentration of trace amounts of water present in the solution of **1** in CD_3CN. The ^1H NMR spectra of samples with increased relative water concentration, at 25 °C, are broader, resulting in different activation parameters. There is a linear relationship between the water concentration and $\Delta G_{pz}^{\ddagger}$; as the water concentration is increasing $\Delta G_{pz}^{\ddagger}$ is decreasing (Figure 10 and 11).

Saturation transfer experiments demonstrated the exchange of the hydrogens between the water in the sample and the bridging hydroxide group, with $\Delta G_{OH}^{\ddagger}$ = 16.8(±0.2) kcal/mol at 25 °C. This value is much larger than the barriers measured for the deprotonation of weak acids (1−2 kcal/mol)[30] and similar to but clearly larger than the barrier of $\Delta G_{pz}^{\ddagger}$ = 15.2(±0.2) kcal/mol for the fluxional process. Supporting the contention that the two processes are independent is the observation of a similar exchange process of the water and the bridging hydroxide group hydrogens in **2** and **3**, complexes for which no exchange of the pyrazolyl rings is observed by NMR. While independent, the two processes are likely related, especially given the similarity of the $\Delta G_{pz}^{\ddagger}$ values for **1**. Clearly the water stabilizes the intermediate in the pseudorotation process more than the ground state, and this interaction could also be involved in the hydrogen exchange.

The $[Zn_2(\mu\text{-OH})(\mu\text{-}\mathbf{L}_m)_2]^{3+}$ complex illustrates that more than one molecular motion can be incorporated into a single molecule (pseudorotation and arene ring flip) through coordination of organic building blocks to metal centers and that these motions can be controlled, similarly to purely organic rotors,[2−4] by substitution of the organic building blocks with bulky groups. In this case, the methyl substitution of the pyrazolyl rings effectively locks the geometry around the metal

dx.doi.org/10.1021/ic402073d | *Inorg. Chem.* 2013, 52, 11638−11649

centers (compounds **2** and **3**). This metallacyclic system also allows the fine-tuning of the barrier to the molecular motion, through careful control of the water concentration in the sample, as water influences the barrier to pseudorotation of the pyrazolyl rings.

5. CONCLUSIONS

The VT-NMR and saturation transfer experiments of $[Zn_2(\mu\text{-}OH)(\mu\text{-}\mathbf{L}_m)_2](ClO_4)_3$ revealed an *unprecedented example of a concerted double Berry pseudorotation for a dinuclear complex*. As imposed by the ligand design, this pseudorotation must be accompanied by the 2-fold flip of the ligand's phenylene spacer along the $C_{methine}$-C_{Ph} bond—we term this process the Columbia Twist and Flip mechanism. The dynamic process that equilibrates the pyrazolyl rings is influenced by the concentration of water in the solvent; in addition, saturation transfer experiments demonstrate that the water hydrogen atoms exchange with the bridging hydroxide hydrogen. We also show that saturation transfer experiments are a valuable method in the determination of $\Delta G^{\ddagger}$ for the fluxional process that equilibrates the pyrazolyl rings in $[Zn_2(\mu\text{-}OH)(\mu\text{-}\mathbf{L}_m)_2](ClO_4)_3$. This method is of general use for the study of coordination compounds that show dynamic processes that may not be completely studied by more conventional variable temperature methods. Compounds $[Zn_2(\mu\text{-}OH)(\mu\text{-}\mathbf{L}_m{}^*)_2](ClO_4)_3$ and $[Cd_2(\mu\text{-}OH)(\mu\text{-}\mathbf{L}_m{}^*)_2](ClO_4)_3$ do not show the dynamic process involving the pyrazolyl-rings in solution because of steric crowding caused by the methyl group substitution, but do show the exchange between the water in the solvent and the bridging hydroxide group.

■ ASSOCIATED CONTENT

Ⓢ Supporting Information

X-ray crystallographic files in CIF format, fully labeled structural diagrams, figure of superimposed structural units, low temperature ^{13}C NMR spectra of $[Zn_2(\mu\text{-}OH)(\mu\text{-}\mathbf{L}_m)_2](ClO_4)_3$. This material is available free of charge via the Internet at http://pubs.acs.org.

Ⓦ Web-Enhanced Feature

A movie animation of Columbia Twist and Flip rearrangement in mpg format is available in the HTML version of the paper.

■ AUTHOR INFORMATION

Corresponding Author

*E-mail: reger@mailbox.sc.edu. Phone: 803-777-2587. Fax: 803-777-9521.

Notes

The authors declare no competing financial interest.

■ ACKNOWLEDGMENTS

The authors acknowledge with thanks the financial support of the National Science Foundation through Grant CHE-1011736 and Filip Stamate for the animation of the Columbia Twist and Flip mechanism.

■ REFERENCES

(1) Selected reviews: (a) Piguet, C. *Chem. Commun.* **2010**, *46*, 6209. (b) Zhang, J.-P.; Huang, X.-C.; Chen, X.-M. *Chem. Soc. Rev.* **2009**, *38*, 2385. (c) Moulton, B.; Zaworotko, M. J. *Chem. Rev.* **2001**, *101*, 1629. (d) Garcia-Garibay, M. A. *Proc. Natl. Acad. Sci.* **2005**, *102*, 10771. (e) Mann, S. *Nat. Mater.* **2009**, *8*, 781.

(2) (a) Kottas, G. S.; Clarke, L. I.; Horinek, D.; Michl, L. *Chem. Rev.* **2005**, *105*, 1281. (b) Skopek, K.; Hershberger, M. C.; Gladysz, J. A. *Coord. Chem. Rev.* **2007**, *251*, 1723. (c) Shirai, Y.; Morin, J.-F.; Sasaki, T.; Guerrero, J. M.; Tour, J. M. *Chem. Soc. Rev.* **2006**, *35*, 1043. (d) Kay, E. R.; Leigh, D. A.; Zerbetto, F. *Angew. Chem., Int. Ed.* **2007**, *46*, 72.

(3) (a) Thanasekaran, P.; Lee, C.-C.; Lu, K.-L. *Acc. Chem. Res.* **2012**, *45* (9), 1403. (b) Rajakannu, P.; Shankar, B.; Yadav, A.; Shanmugam, R.; Gupta, D.; Hussain, F.; Chang, C.-H.; Sathiyendiran, M.; Lu, K.-L. *Organometallics* **2011**, *30*, 3168. (c) Gardinier, J. R.; Pellechia, P. J.; Smith, M. D. *J. Am. Chem. Soc.* **2005**, *127*, 12448. (d) Caskey, D. C.; Michl, J. *J. Org. Chem.* **2005**, *70*, 5442.

(4) (a) Morris, W.; Taylor, R. E.; Dybowski, C.; Yaghi, O. M.; Garcia-Garibay, M. A. *J. Mol. Struct.* **2011**, *1004*, 94. (b) Gould, S. L.; Tranchemontagne, D.; Yaghi, O. M.; Garcia-Garibay, M. A. *J. Am. Chem. Soc.* **2008**, *130*, 3246.

(5) (a) He, C.; Lippard, S. J. *J. Am. Chem. Soc.* **2000**, *122*, 184. (b) Ingle, G. K.; Makowska-Grzyska, M. M.; Arif, A. M.; Berreau, L. M. *Eur. J. Inorg. Chem.* **2007**, 5262. (c) Berreau, L. M.; Allred, R. A.; Makowska-Grzyska, M. M.; Arif, A. M. *Chem. Commun.* **2000**, 1423. (d) Allred, R. A.; McAlexander, L. H.; Arif, A. M.; Berreau, L. M. *Inorg. Chem.* **2001**, *41*, 6790. (e) Bergquist, C.; Parkin, G. *Inorg. Chem.* **1999**, *38*, 422.

(6) (a) Sträter, N.; Lipscomb, W. N.; Klabunde, T.; Krebs, B. *Angew. Chem., Int. Ed.* **1996**, *35*, 2024. (b) Lipscomb, W. N.; Sträter, N. *Chem. Rev.* **1996**, *96*, 2375. (c) Wilcox, D. E. *Chem. Rev.* **1996**, *96*, 2435. (d) Mulder, F. A. A.; Mittermaier, A.; Hon, B.; Dahlquist, F. W.; Kay, L. E. *Nat. Struct. Biol.* **2001**, *8*, 932.

(7) (a) Reger, D. L.; Pascui, A. E.; Smith, M. D.; Jezierska, J.; Ozarowski, A. *Inorg. Chem.* **2012**, *51*, 11820. (b) Reger, D. L.; Foley, E. A.; Watson, R. P.; Pellechia, P. J.; Smith, M. D. *Inorg. Chem.* **2009**, *48*, 10658. (c) Reger, D. L.; Watson, R. P.; Gardinier, J. R.; Smith, M. D.; Pellechia, P. J. *Inorg. Chem.* **2006**, *45*, 10088.

(8) Reger, D. L.; Pascui, A. E.; Smith, M. D.; Jezierska, J.; Ozarowski, A. *Inorg. Chem.* **2012**, *51*, 7966.

(9) Reger, D. L.; Watson, R. P.; Smith, M. D.; Pellechia, P. J. *Organometallics* **2005**, *24*, 1544.

(10) Jarek, R. L.; Flesher, R. J.; Shin, S. K. *J. Chem. Educ.* **1997**, *74*, 978.

(11) (a) Barbour, L. J. *J. Supramol. Chem.* **2003**, *1*, 189. (b) *POV-RAY*, 3.6; Persistence of Vision Raytracer Pty Ltd: Williamstown, Victoria, Australia, 2006.

(12) *MestReNOVA*, v.5.2.5; Mestrelab Research S. L.: Santiago de Compostela, Spain, 2008.

(13) Wolsey, W. C. *J. Chem. Educ.* **1973**, *50*, A335−A337.

(14) *SMART*, Version 5.630, *SAINT+*, Version 6.45; Bruker Analytical X-ray Systems, Inc.: Madison, WI, 2003.

(15) Sheldrick, G.M. *SHELXTL*, Version 6.14; Bruker Analytical X-ray Systems, Inc.: Madison, WI, 2000.

(16) Addison, A. W.; Rao, T. N.; Reedijk, J.; Van Rijn, J.; Verschoor, G. C. *J. Chem. Soc., Dalton Trans.* **1984**, 1349 ; $\tau_5 = (\beta - \alpha)/(60°)$ where α and β are the two largest angles measured around the metal centers. Perfect square pyramid: $\tau_5 = 0$; Perfect trigonal bipyramid: $\tau_5 = 1$.

(17) Shannon, R. D. *Acta Crystallogr.* **1976**, *A32*, 751.

(18) Gavrilova, A. L.; Qin, C. J.; Sommer, R. D.; Rheingold, A. L.; Bosnich, B. *J. Am. Chem. Soc.* **2002**, *124*, 1714.

(19) (a) Valentini, M.; Pregosin, P. S.; Rüegger, H. *Organometallics* **2000**, *19*, 2551. (b) Stilbs, P. *Prog. NMR Spectrosc.* **1987**, *19*, 1.

(20) Sandström, J. *Dynamic NMR Spectroscopy*; Academic Press: London, U.K., 1982.

(21) Marat, K. *SPINWORKS 3*, v.3.1.8.2; University of Manitoba: Winnipeg, Manitoba, Canada, 2011.

(22) (a) Fernández-Moreira, V.; Thorp-Greenwood, F.; Arthur, R. J.; Kariuki, B. M.; Jenkins, R. L.; Coogan, M. P. *Dalton Trans.* **2010**, *39*, 7493. (b) Guerrero, A.; Jalón, F. A.; Manzano, B. R.; Rodríguez, A.; Claramunt, R. M.; Cornago, P.; Milata, V.; Elguero, J. *Eur. J. Inorg. Chem.* **2004**, 549.

(23) (a) Forsén, S.; Hoffman, R. A. *J. Chem. Phys.* **1963**, *39*, 2892. (b) Babailov, S. P.; Krieger, Y. G. *J. Struct. Chem.* **2001**, *42*, 305. (c) DiFranco, S. A.; Maciulis, N. A.; Staples, R. J.; Batrice, R. J.; Odom, A. L. *Inorg. Chem.* **2012**, *51*, 1187. (d) Faller, J. W.; Wilt, J. C. *Organometallics* **2005**, *24*, 5076. (e) Ashby, M. D.; Govindan, G. N.; Grafton, A. K. *J. Am. Chem. Soc.* **1994**, *116*, 4801. (f) Wik, B. J.; Lersch, M.; Krivokapic, A.; Tilset, M. *J. Am. Chem. Soc.* **2006**, *128*, 2682. (g) Rybtchinski, B.; Cohen, R.; Ben-David, Y.; Martin, J. M. L.; Milstein, D. *J. Am. Chem. Soc.* **2003**, *125*, 11041.

(24) Selected references: (a) Pastor, A.; Martínez-Viviente, E. *Coord. Chem. Rev.* **2008**, *252*, 2314. (b) Sabiah, S.; Varghese, B.; Murthy, N. N. *Dalton Trans.* **2009**, 9770. (c) Schalley, C. A.; Müller, T.; Linnartz, P.; Witt, M.; Schäfer, M.; Lützen, A. *Chem.—Eur. J.* **2002**, *8* (15), 3538. (d) Weilandt, T.; Troff, R. W.; Saxell, H.; Rissanen, K.; Schalley, C. A. *Inorg. Chem.* **2008**, *47*, 7588. (e) Uehara, K.; Kasai, K.; Mizuno, N. *Inorg. Chem.* **2010**, *49*, 2008. (f) Jensen, T. B.; Scopelliti, R.; Bünzli, J.-C. G. *Chem.—Eur. J.* **2007**, *13*, 8404. (g) Ferrer, M.; Pedrosa, A.; Rodríguez, L.; Rossell, O.; Vilaseca, M. *Inorg. Chem* **2010**, *49*, 9438. (h) Habermehl, N. C.; Eisler, D. J.; Kirby, C. W.; Yue, N. L.-S.; Puddephatt, R. J. *Organometallics* **2006**, *25*, 2921. (i) Bachechi, F.; Burini, A.; Galassi, S.; Pietroni, B. R.; Tesei, D. *Eur. J. Inorg. Chem.* **2002**, 2086.

(25) (a) Berry, R. S. *J. Chem. Phys.* **1960**, *32*, 933. (b) Cass, M. E.; Hii, K. K.; Rzepa, H. S. *J. Chem. Educ.* **2006**, *83*, 336.

(26) Chisholm, M. H.; Clark, D. L.; Hampden-Smith, M. J. *J. Am. Chem. Soc.* **1989**, *111*, 574.

(27) (a) Bernstein, L. S.; Kim, J. J.; Pitzer, K. S.; Abramowitz, S.; Levin, I. W. *J. Chem. Phys.* **1975**, *62*, 3671. (b) Bernstein, L. S.; Abramowitz, S.; Levin, I. W. *J. Chem. Phys.* **1976**, *64*, 3228. (c) Caliginana, A.; Aquilanti, V.; Burcl, R.; Handy, N. C.; Tew, D. P. *Chem. Phys. Lett.* **2003**, *369*, 335. (d) Wasada, H.; Hirao, K. *J. Am. Chem. Soc.* **1992**, *114*, 16.

(28) Alcock, N. W.; Herron, N.; Moore, P. *J. Chem. Soc., Dalton Trans.* **1978**, 1282.

(29) Morin, T. J.; Merkel, A.; Lindeman, S. V.; Gardinier, J. R. *Inorg. Chem.* **2010**, *49*, 7992.

(30) (a) Li, S. H.; Rasaiah, J. C. *J. Chem. Phys.* **2011**, *135*, 124505. (b) Rose, M. C.; Stuehr, J. E. *J. Am. Chem. Soc.* **1974**, *94*, 5532. (c) Bučko, T.; Benco, L.; Hafner, J.; Ángyán, J. G. *J. Catal.* **2007**, *250*, 171. (d) Chernyshev, A.; Cukierman, S. *Biophys. J.* **2002**, *82*, 182.